Loss of deep cerebellar nuclei neurons in the 3xTg-AD mouse and protection by an anti-Aβ antibody fragment

Gisela Esquerda-Canals*[#1], Joaquim Martí[#1], Geovanny Rivera-Hernández*, Lydia Giménez-Llort[†] and Sandra Villegas*[2]

(*) Protein Folding and Stability Group. Dpt. de Bioquímica i Biologia Molecular (#) Dpt.de Biologia Cel.lular, de Fisiologia i d'Immunologia. Unidad de Citologia i d'Histologia; (†)Dpt.de Psiquiatria i Medicina, i Institut de Neurociències; Universitat Autònoma de Barcelona, Bellaterra, 08193 Barcelona, Spain.

Running title: **3xTg-AD mouse cerebellum protected by scFv-h3D6**

[1] These authors made equally important contributions to this study.

[2] To whom correspondence should be addressed (e-mail sandra.villegas@uab.cat). Departament de Bioquímica i Biologia Molecular, Unitat de Biociències, Universitat Autònoma de Barcelona, 08193 Cerdanyola del Vallès, Spain. Tel. 34 93 5914258, Fax. 34 93 5911264

Abbreviations used: AD, Alzheimer disease; DCN, deep cerebellar nuclei; GCs, ~~granular~~granule cells; PCs, Purkinje cells; scFv, single chain variable Fragment.

Abstract

The therapeutic potential of scFv-h3D6 has recently been shown in the 3xTg-AD mouse. A clear effect on Aβ-oligomers and certain apolipoproteins in the brain was found, but no effect was seen in the cerebellum. Here, cellular vulnerability of the 3xTg-AD cerebellum is described for the first time, together with its protection by scFv-h3D6. Neuron depletion in the DCN was regionally variable and followed a mediolateral axis of ~~affectation~~involvement that was greatest in the fastigial nucleus, lesser in the interpositus, and ~~not occurring~~negligible in the dentate nucleus. ~~Interestingly, a~~ A sole and low intraperitoneal dose of scFv-h3D6 ~~did~~ protect~~ed~~ 3xTg-AD DCN neurons from death. Further studies ~~would provide~~might provide interesting information about both the potential of scFv-h3D6 as a therapeutic agent and the role of the cerebellum in AD.

INTRODUCTION

Alzheimer's Disease International estimated that 36 million people were living with dementia in 2010, with most cases attributable to Alzheimer disease (AD).[1] Projections of the prevalence of the disease indicated that there may be 66 million cases by 2030 and 115 million by 2050. As a consequence, AD is considered to be a twenty-first century pandemic.

Neuritic plaques composed of β-amyloid (βA) peptides, as well as neurofibrillary tangles of hyperphosphorylated tau-protein, are the histopahological hallmarks of AD.[2] Although brain regions are the structures primarily affected in AD, the occurrence of diffuse βA deposits has also been reported in the molecular layer of the cerebellar cortex and, to a lower extent, in the granule cell layer. [3-5] Additionally, Purkinje cell (PC) loss and synaptic dysfunction are heightened as the disease progresses. [6-9]

The triple-transgenic mouse model of AD (3xTg-AD), harboring two human transgenes causing early onset AD ($PS1_{M146V}$ and APP_{Swe}) and a mutant form of tau (tau_{P301L}), mimics both βA plaques and tau neurofibrillary tangles following a regional and temporal ~~affectation~~involvement homologous to humans. [10] At 4 months of age, βA accumulates in cortical regions and initiates progression to the hippocampus, whereas tau hyperphosphorylation develops after βA accumulation (at ~ 12-15 months), beginning in limbic structures and extending later through cortical regions. [10-12] Since the Alzheimer's Disease International 2011's report claimed the necessity for early intervention in AD, [13] our studies were performed with 5-month-old animals. Females were selected because they exhibit significantly greater Aβ burden and larger behavioral deficits than age-matched males. [14]

We recently used this model to show that immunotherapy with an anti-Aβ antibody fragment is a potential tool for the treatment of AD (Ref. FENS & Giménez-Llort submitted to MAbs). Specifically, we constructed a single-chain variable fragment

(scFv), scFv-h3D6, [15] from the humanized monoclonal antibody AAB-001 (mAb-h3D6, bapineuzumab). [16] An advantage of the use of such fragments compared to the use of complete antibodies is that Fc-mediated activation of microglia cannot occur. Therefore, use of scFv-h3D6 could avoid some of the undesirable effects reported in Phase 3 clinical trials for bapineuzumab. [17] In fact, a single intraperitoneal dose of scFv-h3D6 reversed BPSD-like behaviors, improved long- and short-term learning and memory deficits, globally decreased Aβ-oligomers in the cortex and olfactory bulb, and recovered the non-pathological levels of some apolipoproteins in the cortex (apoE and apoJ) and hippocampus (apoE) (Ref. FENS & Giménez-Llort submitted to MAbs). However, no differences in the concentration of these molecules were found in the cerebellum.

Since affectationinvolvement of human cerebellum has being described in late phases of the disease, we wondered when neuronal vulnerability in the 3xTg-AD cerebellum, either in the cortex or the deep nuclei, could appear. A dramatic death in young 3xTg-AD deep cerebellar nuclei neurons was found and, more interestinglyexciting, we successfully tested the capability of scFv-h3D6 for preventing it.

RESULTS

The numbers of granule cells (GCs) and Purkinje cells (PCs), as well as cellular density, in each cerebellar cortex region analyzed were similar between 3xTg-AD and NTg mice (Table 1). However, differences were found when comparing the area of GCs' layer at the vermis of the untreated (or treated) NTg with that of the untreated 3xTg-AD animals (Table 1), which showed a mild, although significant, decrease. It is noteworthy that scFv-h3D6 treatment exerted a protective effect on the size of GCs' layer because no differences were found between treated 3xTg-AD group and NTg groups.

Similarly, the areas of the fastigial and interpositus nucleus were smaller in the 3xTg-AD mice than in the NTg one, but no differences were found in the dentate nuclei (Table 1). These differences also occurred, and in the same direction, when both cell number and cell density were compared (Table 1). Since changes are bigger in the cell number than in the areas, we below refer to the total number of cells rather than to the cell density.

~~could did not exert an effect in the cerebellar cortex.~~

In contrast to the cerebellar cortex, the loss of neurons was dramatically evident at the cerebellar nuclei (Fig. 1 and Table 1). The number of neurons in the fastigial nucleus was significantly lower in the 3xTg-AD group, with a mean value 24% that of the NTg mice (p=0.050). ~~Interestingly, t~~The treatment with scFv-h3D6 allowed for the maintenance of 61% of the cells of the 3xTg-AD compared to the untreated NTg (p=0.028), and 67% compared to the treated NTg (p=0.014). No significant difference was found between treated and untreated NTg groups. In any case, it is ~~fairly~~ clear that scFv-h3D6 treatment protected fastigial nucleus neurons from death, although its beneficial effect did not reach non-pathological conditions. Photomicrographs of sagittal

sections at the level of the fastigial nucleus show the ~~affectation~~involvement of these DCN neurons and the ~~robust~~pronounced action of scFv-h3D6 on cell viability (Fig. 2).

When cell counts were done in the interpositus nucleus, a similar effect was found (Fig. 1 and Table 1). The cell bodies percentage in the 3xTg-AD was 58% that of the NTg (*p*=0.014), whereas treatment allowed for the survival of 87% of the cells. This value is not significantly different to the initial cell count (untreated NTg) (*p*=0.243) and, in consequence, a complete protection of neurotoxicity could be interpreted. Although the treated NTg group showed higher cell viability that the untreated one (127%), there was no significant difference among these experimental groups (*p*=0.114). As a consequence, scFv-h3D6 treatment completely protected interpositus nucleus neurons from death in the 3xTg-AD mouse. Photomicrographs of sagittal sections at the level of the interpositus nucleus show the ~~affectation~~involvement of these DCN neurons and the recovery of cell viability by scFv-h3D6 (Fig. 2).

When the dentate nucleus was considered, no significant effect of the genotype on the number of neurons was observed (Fig. 1 and Table 1). In consonance, treatment ~~could~~ did not exert an effect in this ~~area~~region.

Several conclusions emerged from these data: (I) the loss of cells in the 3xTg-AD cerebellum depends on the neuronal type examined; (II) macroneuron depletion in the DCN was regionally variable, being greatest in the fastigial nucleus, lesser in the interpositus, and ~~not occurring~~negligible in the dentate nucleus; (III) the administration of scFv-h3D6 protected 3xTg-AD DCN neurons from death, as seen five days after injection of a single dose; and (IV) although the single injection of 100 μg of scFv-h3D6 completely rescued 3xTg-AD interpositus neurons to the level of the NTg mice, this dose was not sufficient to completely rescue fastigial neurons, which were the most affected initially.

6

DISCUSSION

We had previously shown that an antibody fragment, the single-chain variable fragment scFv-h3D6, has the ability to prevent the toxicity induced by the Aβ peptide in human neuroblastoma cell-cultures.[15] Additionally, we recently demonstrated the benefits of scFv-h3D6 in 5-month-old female 3xTg-AD animals, which corresponds to early stages of the disease (Ref. FENS & Giménez-Llort submitted to MAbs).

The 3xTg-AD mouse brain develops molecular and histological alterations characteristic of AD, following a regional and temporal ~~affectation~~involvement homologous to humans. [10,] [18] Because some studies revealed the ~~affectation~~involvement of cerebellum in late phases of the disease, [5] study of the disease progression in the 3xTg-AD mouse's cerebellum is of interest. Other mouse models that are also linked to PS1 mutations showed cerebellar Aβ deposition in the form of neuritic plaques and Purkinje cell loss. [19] A few Aβ plaques were detected in the molecular layer at 6 months, but loss of synaptic contacts between parallel fibers and dendritic spines of Purkinje cells, and degeneration of granule cells, required 12 months.

Although cerebellar neurons have been reported to be more resistant to soluble oligomeric Aβ than other neurons in the brain, we wondered when neuronal vulnerability in the 3xTg-AD cerebellum could appear. We focused the study in both the cerebellar cortex and deep nuclei by counting different cellular populations. Plausibly, we did not observe significant differences in the cerebellar cortex because we studied a very early stage of the disease progression. In contrast, the 3xTg-AD cerebellar nuclei showed a gradient of neural loss through the mediolateral axis, with the fastigial nucleus the most affected area, followed by the interpositus nucleus, and dentate nucleus not being affected. Although several studies have demonstrated the direct

anatomic connection from fastigial nucleus to encephalic regions as ~~amygdale~~amygdala, hippocampus and cerebral cortex, [20] as well as the projection through thalamus of interpositus and dentate nucleus to cerebral cortex, [21] this is the first time that deep cerebellar nuclei neurons are shown to be affected at early stages of AD progression.

Even more exciting, however, is the finding that scFv-h3D6 is able to protect 3xTg-AD DCN neurons from death~~n~~, although the extent of protection was variable. While administration of scFv-h3D6 completely rescued 3xTg-AD interpositus neurons to the non-pathological level of the NTg mice, this dose was not sufficient to completely rescue fastigial neurons, which were initially the most affected ones. It is important to note that, in contrast to other published studies, i.e., intranasal administration of 1.5 mg/ml scFv twice a week for 14 weeks, [22] in the current work 100 μg of scFv-h3D6 were intraperitoneally administered and the effect assessed five days after this low and sole dose.

In conclusion, we described the Aβ-induced death of deep cerebellar nuclei neurons at early stages of the disease progression in the 3xTg-AD mouse model and their rescue by a single, low dose of scFv-h3D6. Further studies increasing dose and using other stages of the disease ~~would provide~~might provide interesting information about both the therapeutic potential of scFv-h3D6 and the role of the cerebellum in Alzheimer disease.

MATERIALS AND METHODS

ScFv-h3D6 was recombinantly expressed in *E. coli* and purified as previously described (Rivera-Hernández submitted to MAbs). Lipopolysaccharides (LPS), the major endotoxins of gram-negative bacteria, were removed from the protein by using Detoxi-Gel Endotoxin Removing columns (Thermo Scientific).

Triple-transgenic 3xTg-AD mouse harboring $PS1_{M146V}$, APP_{Swe} and tau_{P301L} transgenes was genetically engineered at the University of California Irvine. [10] Sixteen 5-month-old females animals from the Spanish colony of homozygous 3xTg-AD and wild-type non-transgenic (NTg) mice [23] (n=8 each group) were used in the present study. Standard laboratory conditions (food and water *ad lib*, 22 ± 2 ºC, 12 h light: dark cycle starting at 08:00) were used and all the experiments were carried out in accordance with the requirements of the Ethical Committee of Universitat Autònoma de Barcelona.

Animals were randomly treated with a single intraperitoneal dose of 100 µg scFv-h3D6 or vehicle (PBS-buffer) (n=4). After five days, animals were anesthetized with sodium pentobarbital (50 mg/kg) and perfused through the heart with 4% paraformaldehyde in PBS-buffer (pH 7.4). Tissue processing was developed as regular procedures from our laboratory. [24] The blocks containing the cerebellum were sectioned serially at 10 µm in the sagittal plane and one of every six sections was saved. Sections were stained with hematoxylin-eosin or cresyl violet.

~~Neurons were counted in representative sections of every mediolateral parcellation of the cerebellar cortex separately: vermis, paravermis, and hemispheres. GCs and PCs were scored in lobules (I to X) at vermis and paravermis, whereas simplex, ansiform and paramedian lobules were considered at the hemispheres. In the deep cerebellar nuclei (DCN), macroneurons (body cell bigger than 20 µm in diameter) were separately counted at the level of the fastigial, interpositus and dentate nucleus.~~ The number of GCs and PCs were counted separately in vermis and paravermis (lobules I to X). Criteria for scoring them included both morphological and staining properties. Small, darkly stained and densely packed cells were considered as GCs. PCs were counted on the bases of several assumptions such as size, the morphological characteristics of the pericarion and distinctive stain properties. These macroneurons were considered as present if they possessed large pear-shape cell body and nucleus with the presence of a distinct nucleolus.

The quantity of deep nuclear neurons was independently determined at the level of the fastigial, the interpositus and the dentate nuclei. Quantification of DCN neurons deserves special attention because it is known that two cellular types, small and large, coexist. To obtain reliable data, those neurons with a cell body smaller than 20 μm in diameter were rejected.

Photographic material was digitally captured by a CCD-IRIS color video camera (Sony, Japan) coupled to a Zeiss Axiosphot microscope. The digitized images were processed with the Adobe Photoshop software.

The statistical significance of the results was evaluated with the non-parametric Mann-Whitney *U*-test. A "*p*" value equal or lower than 0.05 was considered statistically significant.

The authors state that "there are no potential conflicts of interest in our submission".

References

1. Alzheimer's Disease International. World alzheimer's report 2009: The global prevalence of dementia. 2009.

2. Selkoe DJ. Alzheimer's disease results from the cerebral accumulation and cytotoxicity of amyloid beta-protein. J Alzheimers Dis 2001; 3:75-80.

3. Li YT, Woodruff-Pak DS, Trojanowski JQ. Amyloid plaques in cerebellar cortex and the integrity of purkinje cell dendrites. Neurobiol Aging 1994; 15:1-9.

4. Selkoe DJ. Normal and abnormal biology of the beta-amyloid precursor protein. Annu Rev Neurosci 1994; 17:489-517.

5. Thal DR, Rub U, Orantes M, Braak H. Phases of A beta-deposition in the human brain and its relevance for the development of AD. Neurology 2002; 58:1791-800.

6. Fukutani Y, Cairns NJ, Rossor MN, Lantos PL. Cerebellar pathology in sporadic and familial alzheimer's disease including APP 717 (val-->Ile) mutation cases: A morphometric investigation. J Neurol Sci 1997; 149:177-84.

7. Lemere CA, Lopera F, Kosik KS, Lendon CL, Ossa J, Saido TC, et al. The E280A presenilin 1 alzheimer mutation produces increased A beta 42 deposition and severe cerebellar pathology. Nat Med 1996; 2:1146-50.

8. Giaccone G, Morbin M, Moda F, Botta M, Mazzoleni G, Uggetti A, et al. Neuropathology of the recessive A673V APP mutation: Alzheimer disease with distinctive features. Acta Neuropathol 2010; 120:803-12.

9. Sepulveda-Falla D, Matschke J, Bernreuther C, Hagel C, Puig B, Villegas A, et al. Deposition of hyperphosphorylated tau in cerebellum of PS1 E280A alzheimer's disease. Brain Pathol 2011; 21:452-63.

10. Oddo S, Caccamo A, Shepherd JD, Murphy MP, Golde TE, Kayed R, et al. Triple-transgenic model of alzheimer's disease with plaques and tangles: Intracellular abeta and synaptic dysfunction. Neuron 2003; 39:409-21.

11. Clinton LK, Billings LM, Green KN, Caccamo A, Ngo J, Oddo S, et al. Age-dependent sexual dimorphism in cognition and stress response in the 3xTg-AD mice. Neurobiol Dis 2007; 28:76-82.

12. Mastrangelo MA, Bowers WJ. Detailed immunohistochemical characterization of temporal and spatial progression of alzheimer's disease-related pathologies in male triple-transgenic mice. BMC Neurosci 2008; 9:81,2202-9-81.

13. Alzheimer's Disease International. World alzheimer report 2011: The benefits of early diagnosis and intervention. 2011.

14. Carroll JC, Rosario ER, Kreimer S, Villamagna A, Gentzschein E, Stanczyk FZ, et al. Sex differences in beta-amyloid accumulation in 3xTg-AD mice: Role of neonatal sex steroid hormone exposure. Brain Res 2010; 1366:233-45.

15. Marin-Argany M, Rivera-Hernandez G, Marti J, Villegas S. An anti-abeta (amyloid beta) single-chain variable fragment prevents amyloid fibril formation and cytotoxicity by withdrawing abeta oligomers from the amyloid pathway. Biochem J 2011; 437:25-34.

16. Panza F, Frisardi V, Imbimbo BP, Seripa D, Paris F, Santamato A, et al. Anti-beta-amyloid immunotherapy for alzheimer's disease: Focus on bapineuzumab. Curr Alzheimer Res 2011; 8:808-17.

17. Panza F, Frisardi V, Solfrizzi V, Imbimbo BP, Logroscino G, Santamato A, et al. Immunotherapy for alzheimer's disease: From anti-beta-amyloid to tau-based immunization strategies. Immunotherapy 2012.

18. Oddo S, Caccamo A, Kitazawa M, Tseng BP, LaFerla FM. Amyloid deposition precedes tangle formation in a triple transgenic model of alzheimer's disease. Neurobiol Aging 2003; 24:1063-70.

19. Lomoio S, Lopez-Gonzalez I, Aso E, Carmona M, Torrejon-Escribano B, Scherini E, et al. Cerebellar amyloid-beta plaques: Disturbed cortical circuitry in AbetaPP/PS1 transgenic mice as a model of familial alzheimer's disease. J Alzheimers Dis 2012; 31:285-300.

20. Heath RG, Harper JW. Ascending projections of the cerebellar fastigial nucleus to the hippocampus, amygdala, and other temporal lobe sites: Evoked potential and histological studies in monkeys and cats. Exp Neurol 1974; 45:268-87; PMID: 4422320.

21. Delgado-Garcia JM. Structure and function of the cerebellum. Rev Neurol 2001; 33:635-42.

22. Cattepoel S, Hanenberg M, Kulic L, Nitsch RM. Chronic intranasal treatment with an anti-abeta(30-42) scFv antibody ameliorates amyloid pathology in a transgenic mouse model of alzheimer's disease. PLoS One 2011; 6:e18296.

23. Giménez-Llort L, Blázquez G, Cañete T, Rosa R, Vivó M, Oddo S, et al. Modeling neuropsychiatric symptoms of Alzheimer's disease dementia in 3xTg-AD mice. In: *Alzheimer's Disease: New Advances*. Iqbal K, Winblad B, Avila J, eds. Pianoro (BO), Italy: Medimond SRL,eds., 2006:513-516.

24. Marti J, Santa-Cruz MC, Serra R, Valero O, Molina V, Hervas JP, et al. Principal component and cluster analysis of morphological variables reveals multiple discrete sub-phenotypes in weaver mouse mutants. Cerebellum 2013; 12:406-17.

 LEGENDS TO FIGURES

Figure 1: Depletion of deep cerebellar nuclei neurons in the 3xTg-AD mouse cerebellum and recovery by scFv-h3D6 treatment. Cell numbers from fastigial, interposed and dentate nuclei were determined. Black, untreated NTg group; Striped, scFv-treated NTg group; White, untreated 3xTg-AD group; Squared, scFv-treated 3xTg-AD group. Results are expressed by means ± S.E.M. *significant *vs* untreated NTg group (p≤0.05); **significant *vs* untreated 3xTg-AD group (p<0.03). Significance values were calculated via Mann-Whitney test.

Figure 2: Illustrative photomicrographs of sagittal sections. At the level of the fastigial and interpositus nuclei the ~~affectation~~involvement of DCN neurons and its protection by scFv-h3D6 is shown. Bar is 50 µm.

LEGENDS TO TABLES

Table 1: Numerical values of the neuronal populations from cerebellar cortex and nuclei (PC, GC and DCN macroneurons) quantification.

Cell number, area (mm^2), and density (number of cells/mm^2) were quantified. Results are expressed by means ± S.E.M. *significant *vs* untreated NTg group (p≤0.05); **significant *vs* untreated 3xTg-AD group (p≤0.05). Treated NTg significances vs other groups are omitted as no significant effects were found upon treatment. Significance values were calculated via Mann-Whitney test. [a]Length refers to that of the monolayer (Purkinje Cells Layer) in mm and cellular density refers the number of PC per unit of length.
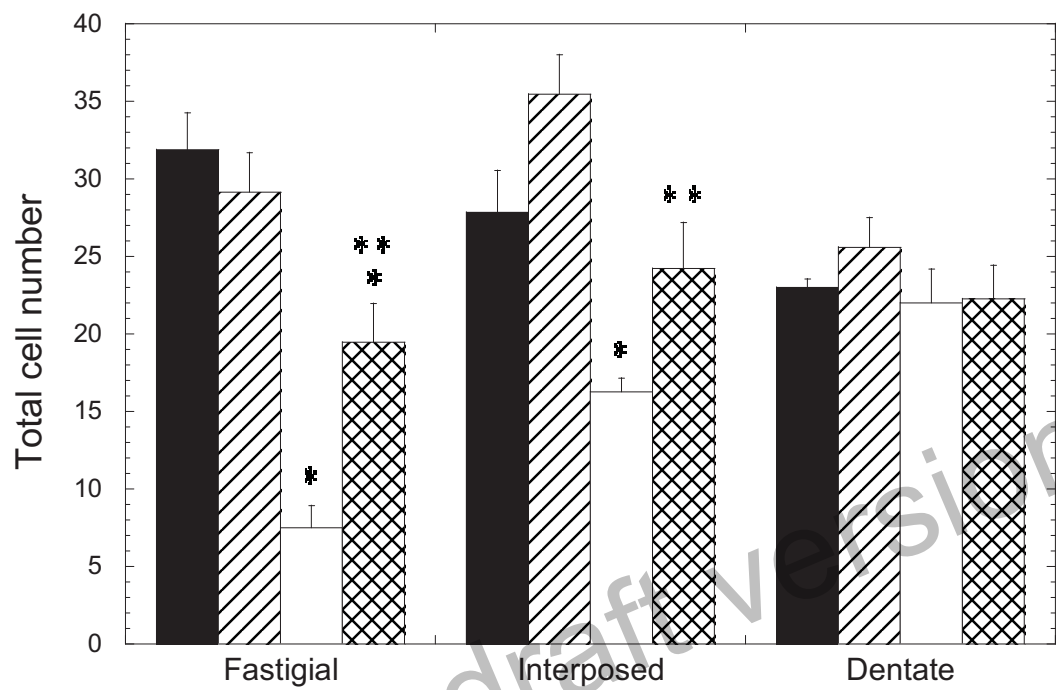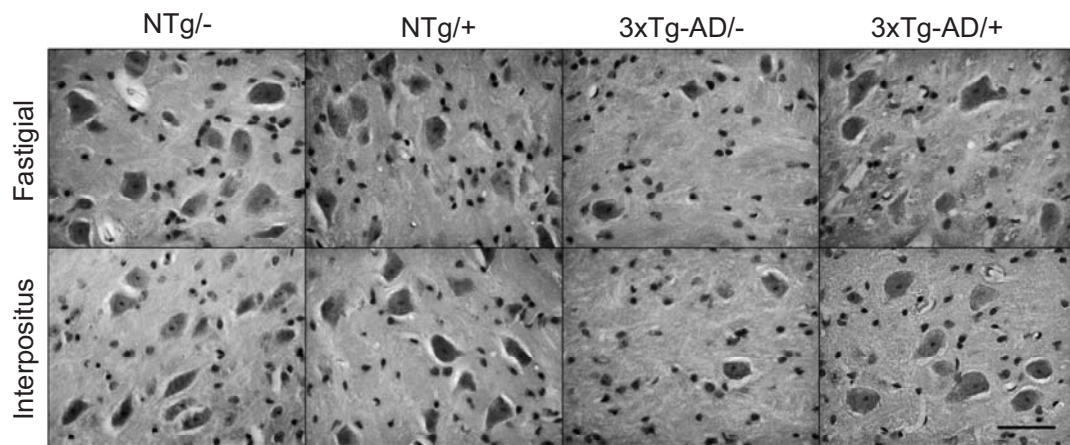
14

FIGURE 1

FIGURE 2

Table 1

	NTg/-	NTg/+	3xTg-AD/-	3xTg-AD/+
Purkinje cells				
Vermis				
Cell number	788.5±20.5	748.5±53.9	758.3±35.5	789.3±36.3
Length[a]	27.3±0.5	27.1±0.5	24.7±1.5	28.3±0.9
Cellular density[a]	28.9±0.5	27.5±1.7	30.8±1.6	27.9±1.1
Paravermis				
Cell number	685.5±58.6	725.5±36.9	706.3±39.6	681.3±16.9
Length[a]	24.9±2.1	25.1±0.8	24.7±1.0	26.1±0.6
Cellular density[a]	27.6±0.3	29.0±1.8	28.6±0.8	26.1±0.6
Granule cells				
Vermis				
Cell number	58192±3464	56312±178	47815±2634	56389±2085
Area	3.4±0.2	3.4±0.0	2.9±0.0*	3.2±0.1**
Cellular density	17214±237	16827±127	16608±626	17581±513
Paravermis				
Cell number	41946±4850	40263±2553	42010±4619	44609±3625
Area	2.8±0.0	2.4±0.0	2.6±0.1	2.7±0.1
Cellular density	15024±592	16807±932	16145±650	16297±1012
DCN macroneurons				
Fastigial				
Cell number	31.89±2.35	29.13±2.53	7.50±1.44*	19.46±2.50*/**
Area	0.37±0.04	0.35±0.03	0.15±0.01*	0.27±0.03**
Cellular density	88.61±7.98	82.96±2.62	60.44±1.08*	71.06±3.76**
Interpositus				
Cell number	27.83±2.73	35.47±2.53	16.25±0.89*	24.23±2.96**
Area	0.49±0.05	0.57±0.04	0.36±0.02*	0.46±0.02**
Cellular density	57.20±2.26	62.81±5.85	44.86±1.77*	56.30±3.11**
Dentate				
Cell number	22.89±1.82	25.58±1.94	22.00±2.18	22.25±2.15
Area	0.35±0.04	0.41±0.01	0.37±0.03	0.38±0.05
Cellular density	66.47±2.34	62.04±5.26	59.39±1.54	62.54±10.08